

Modeling DT Vaporization and Melting in a Direct Drive Target

B. R. Christensen¹, A. R. Raffray¹, M. S. Tillack¹

¹Mechanical and Aerospace Engineering Department and Center for Energy Research, University of California, San Diego, La Jolla, CA 92093-0438

Abstract

During injection, inertial fusion energy (IFE) direct drive targets are subjected to heating from energy exchange with the background gas and radiation from the reactor wall. This thermal loading could cause phase change (vaporization and/or melting) of the deuterium-tritium (DT). In the past, it was assumed that any phase change would result in a violation of the stringent smoothness and symmetry requirements imposed on the target. This work summarizes the results from a one-dimensional finite difference model that was created to simulate the coupled thermal and mechanical response of a direct drive target to an imposed heat flux.

The objective of this work is to investigate the potential of allowing targets to undergo phase change.

Introduction

The IFE direct drive concept utilizes multiple laser beams to compress and heat small spherical targets loaded with fusion fuel (see fig. 1), resulting in a fusion micro-explosion. Initial perturbations in the target, caused by surface roughness, vapor bubbles, or other inconsistencies, must be minimized to maximize the implosion efficiency [1-5].

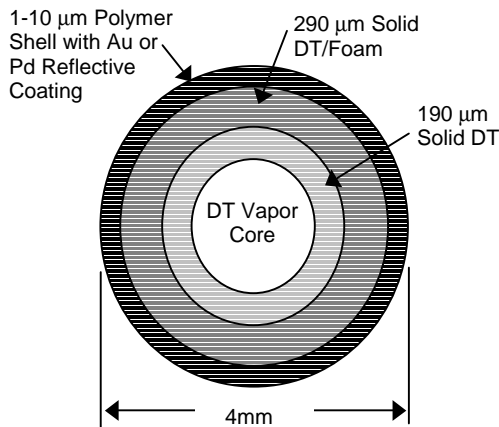


Figure 1. The cross-section of a typical direct drive IFE target considered in this study (not to scale).

For IFE to be successful an acceptable target must be presented at the center of the reaction chamber at approximately 10 Hz. Previously, it was assumed that the maximum DT temperature must remain below the

triple point, $T_{TP,DT}$, for a target to remain viable [6]. This criterion assumes that DT phase change would violate the stringent smoothness, symmetry, and/or continuity requirements placed on the target. It also assumes that sublimation, which occurs below the triple point, will not result in violations of acceptance criteria.

Many commercial software packages are suitable for modeling the temperature distribution in a direct drive target subjected to a heat flux; however, the ability to couple the mechanical response (thermal expansion, deflection due melting and vapor formation) with the thermal response (heat conduction, phase change) is not readily available. Therefore, an integrated thermomechanical model was created that incorporated each of the important processes so that the consequences of phase change could be studied.

Other work has focused on characterizing the thermal loading of a direct drive target as it travels through an IFE reaction chamber environment [7,8]. The ability to model the heat loading produced by various chamber environments, and the response of various target designs to those environments, allows for an integrated target-chamber design to be pursued.

Assumptions used in the thermomechanical model

For this initial attempt to model the thermal and mechanical response of a direct drive target, several simplifying assumptions are made.

One-dimensional heat transfer – Solution of the energy equation allows for the determination of the minimum time to reach $T_{DT,TP}$ and/or the maximum amount of phase change.

Uniform and constant DT mechanical properties – The elastic modulus of DT (E_{DT}) is based on data for D_2 as given in Souers [9]. The changing thickness of the solid DT shell due to phase change is included in the model.

Continuous DT vapor layer – In actual targets vaporization will probably occur as bubble formation (boiling) at the polymer/DT interface. To simplify the model, while retaining some of the effects of DT vaporization, it is assumed that a vapor layer exists over the entire DT-polymer interface (fig. 2). This simplifies both the heat conduction equation and the calculation of the deflection of the polymer and DT shells.

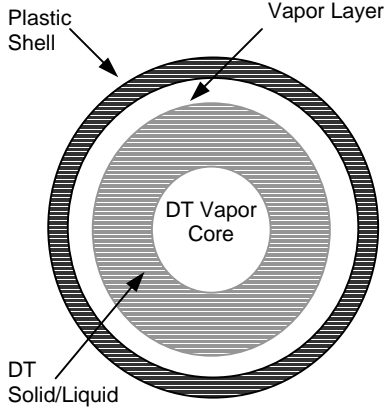


Figure 2. The cross-section of a direct drive target with a uniform vapor layer.

Continuum thermal resistance of DT vapor - When DT vapor is present it is assumed to behave as a linear thermal resistor, where heat transfer takes place only by continuum conduction through the DT vapor.

A simple calculation shows that for vapor layers with thickness $< 1 \mu\text{m}$, the DT vapor operates in the transition or slip regime. In these regimes the thermal conductivity of the vapor will be significantly lower than the continuum value [10].

Neglect of thermal effect of evaporation and sublimation - Several cases, with and without the apparent heat sink resulting from evaporation and sublimation at the surface of the DT solid/liquid, were executed. A comparison of the results showed that evaporation/sublimation does not represent a significant thermal effect over the range of expected incident heat flux. By neglecting the non-linear interface condition introduced by evaporation and/or sublimation, the computation time is decreased by approximately five times.

DT vapor is an ideal gas - The validity of the ideal gas assumption fades as the critical point or saturation line (see Souers for saturation data [9]) is approached [11]. Since the vapor pressure and temperature in a target could be at or near the critical point or saturation line, the compressibility factor should be included in future models.

The integrated thermomechanical model

The thermal and mechanical response of a target is mainly coupled through melting and vaporization. The increase in specific volume, attendant with melting/vaporization, causes the polymer shell and DT solid to deflect. Since the viability of the target is related to its continuity and symmetry, it is essential to predict the amount and type of phase change that will occur as a target is heated. Many methods, of varying complexity, exist for modeling melting [12]. A simple

method for modeling melting phase change, called the apparent c_p method, is used in this model. Kinetic theory is used to calculate the rate of vaporization, and hence the pressure in the vapor layer (if applicable).

Basic equations

To account for the rapid change in thermal properties at temperatures in the cryogenic region, and to model melting, the heat conduction equation with variable properties is used. The 1-d heat conduction equation, in spherical coordinates, is given (in expanded form) as:

$$\frac{\partial T}{\partial t} = \frac{1}{\rho c_p(T)} \left[\frac{\partial T}{\partial r} \left(\frac{2k}{r} + \frac{\partial k}{\partial r} \right) + k \frac{\partial^2 T}{\partial r^2} \right] \quad (1)$$

where T is the temperature (K), ρ is the density (kg/m^3), c_p is the heat capacity (J/kg-K), k is the thermal conductivity (W/m-K), and t is time (s).

Eq. 1 was discretized and solved using the forward time central space (FTCS) finite difference method. The thermal properties at time $n+1$ were estimated, at time n , using extrapolation. Ozisik [12] describes more complex and accurate methods of determining thermal properties at time $n+1$.

Boundary and interface conditions

The boundary condition at the outer surface of the target is assumed to be a constant heat flux. The boundary between the DT solid and the DT vapor core (fig. 1) is assumed to be adiabatic.

The interface condition applied at the interface of different materials, and across the vapor layer, (if present) is of the form:

$$-k_a \frac{\partial T}{\partial r} = h(T_a^{n+1} - T_b^{n+1}) \quad (2)$$

where h is the heat transfer coefficient across the boundary.

When a vapor layer is present between the inner surface of the polymer shell and the outer surface of the DT solid/liquid, it is essential to know the thickness of the vapor layer to determine h . The vapor layer thickness is completely determined by the pressure in vapor layer, which is determined by the density and temperature of the vapor. The vaporization of DT can be simply modeled using kinetic theory [13]. The net mass flux leaving the DT surface due to condensation or evaporation is given by:

$$j = \left(\frac{M}{2\pi R} \right)^{1/2} \left[\frac{p_{sat}}{T_{surface}^{1/2}} - \frac{p_{vap}}{T_{vap}^{1/2}} \right] \quad (3)$$

where p_{sat} is the saturation pressure of the DT (Pa), p_{vap} is the pressure of the DT vapor in the vapor layer, T_{vap} is the vapor temperature (K), and T_s is the temperature (K) of the DT surface where vaporization/condensation occurs.

By assuming that the DT vapor behaves as an ideal gas, and that the vapor filled volume is approximately constant for a small time step, Eq. 3 can be integrated in time to give the mass in the vapor layer at the end of a small time step.

For the conditions appropriate to this problem, it is easily shown that the vapor will be saturated (zero net mass flux) by the end of a time step, when the time step is larger than $\sim 0.1 \mu\text{s}$.

Since the vapor is saturated at time $n+1$, the mass flux (Eq. 3) must equal zero; therefore, the pressure in the vapor layer at $n+1$ is given by:

$$p_{vap} = p_{sat} \left(\frac{T_{vap}^{1/2}}{T_s^{1/2}} \right). \quad (4)$$

The vapor pressure resulting from Eq. 4 is used to find the deflection of the polymer and DT; hence the thickness of the vapor layer at each time step.

Now the heat transfer coefficient (to be used in Eq. 2) across the vapor layer is given by:

$$h = \frac{k_{vap}}{\lambda} \quad (5)$$

where k_{vap} (W/m-K) is the thermal conductivity of the DT vapor, and λ (m) is the average vapor layer thickness over the time n to $n+1$. If no vapor layer exists h is based on the contact resistance of the DT solid/liquid on the polymer.

When vapor is present it is necessary to account for the fact that the vapor layer thickness changes over each time step. An iteration scheme is used to determine the appropriate λ .

Modeling deflection

The deflection of the thin polymer shell, subjected to a uniform internal pressure, is calculated using membrane theory as [14]:

$$\delta_{polymer} = \frac{pr_{pol}^2(1-\nu_{pol})}{2E_{pol}t_{pol}} \quad (6)$$

where p (Pa) is the uniform internal pressure, r_{pol} (m) is the radius of the polymer shell, ν_{pol} is Poisson's ratio for the polymer, E_{pol} (Pa) is the elastic modulus for the polymer, and t_{pol} (m) is the thickness of the polymer shell.

The deflection of the outer surface of a uniformly loaded thick spherical shell (DT solid) is given by [15]:

$$\Delta r_a = \frac{-pr_a}{E_{DT}} \left[\frac{(1-\nu_{DT})(r_b^3 + 2r_a^3)}{2(r^3 - r_b^3)} - \nu_{DT} \right] \quad (7)$$

where r_a (m) and r_b (m) are the radii of the outer and inner surface respectively, E_{DT} is the elastic modulus for DT (Pa), and ν_{DT} is Poisson's ratio for DT.

Modeling solid-to-liquid phase change

A simple, approximate method is used to account for melting in the DT. This method is implemented by defining an apparent specific heat (c_p) for the DT. In general c_p is defined as:

$$c_p = \frac{d\eta}{dT} \quad (8)$$

where η is the specific enthalpy (J/kg), and T is the temperature (K). As with all pure substances, the enthalpy of DT jumps at $T_{TP,DT}$ (the triple point

temperature of DT), causing Eq. 8 to be infinite at $T_{TP,DT}$. Bonacina [16] reported that a good engineering approximation of phase change is made by assuming that phase change takes place over a small temperature range ΔT_{pc} that contains $T_{TP,DT}$. Over the phase change interval ΔT_{pc} , the apparent c_p is taken as [16]:

$$c_p^* = \frac{L_f}{\Delta T_{pc}}. \quad (9)$$

The apparent c_p method stems from the analysis of alloys, where phase change actually occurs over a small temperature range. When applying this method to a finite difference model Bonacina [16] noted that the best results are obtained when at least 2-3 nodes are in the "melting" region (that is the node temperatures are in the range ΔT_{pc}) at each time step. If the thermal conductivity jumps at the triple point it is necessary to assume that the thermal conductivity changes over the small temperature range ΔT_{pc} in order for this method to function properly.

Modes of vaporization

Several modes of vapor production can occur depending on the conditions. The modes of vapor growth that could occur inside of a target are homogeneous and heterogeneous nucleation

Heterogeneous nucleation occurs at a preexisting vapor filled nucleation sites. For DT the critical radius of a nucleation site (the radius below which nucleation will not occur) is $\sim 0.5 \mu\text{m}$ at 19 K, and $0.1 \mu\text{m}$ at 22 K. The presence of helium-3 or other dissolved gas will decrease the critical radius [19,20]. The small critical radius suggests that heterogeneous nucleation is likely.

Homogeneous nucleation is the spontaneous creation of vapor nuclei without the aid of preexisting nucleation sites. In *Boiling Phenomena* [20] it is shown that homogeneous nucleation occurs very slowly for temperatures less than $0.9T_c$ (where T_c is the critical temperature of the fluid). Above $0.9T_c$ the creation of vapor nuclei is extremely rapid. The presence of helium-3 will increase the rate of spontaneous nucleation according to its concentration [20]. Since the helium-3 concentration is unknown, $0.8T_c$ is taken as the maximum allowable DT temperature.

Validating the thermomechanical model

The validity of the thermomechanical model was tested throughout its development by comparing the numerical results to results from exact solutions for simplified cases (i.e., constant thermal properties, no phase change). In addition, the conservation of energy was continuously checked and satisfied by the model. To test the validity of the melting model, an analytical solution was derived. The results of the analytical solution and the numerical model are compared below.

There are few analytical solutions to the melting problem; however, some solutions for simplified geometries and boundary conditions do exist. These analytical solutions can be compared to the numerical

model to test the validity of the apparent c_p method discussed earlier.

To examine the performance of the present spherical model, an analytical solution for a solid sphere undergoing phase change was derived based on a solution for a semi-infinite slab [17]. The results from the analytical solution are compared to the numerical results below.

Fig. 3 shows that the solution (melt layer thickness as a function of time) converges as the node spacing (Δr) is decreased. Similar tests show that the results converge as the time step is decreased.

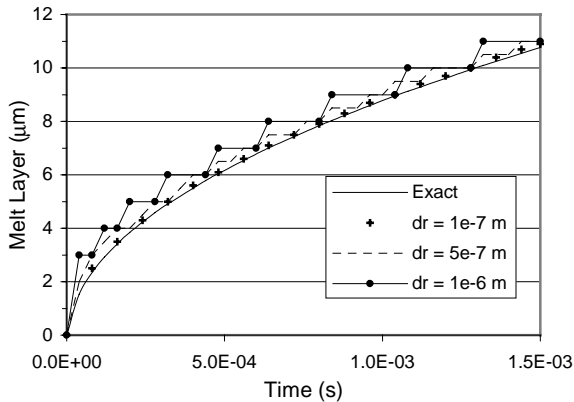


Figure 3. Decreasing Δr increases the accuracy of the numerical solution.

While it appears that the apparent c_p approach can adequately track the melt layer thickness, this is not the only measure of accuracy for the numerical model. Another metric is the ability to model the transient temperature field.

Fig. 4 shows the temperature field at $t = 1.5$ ms for a cases where $\Delta r = 1 \mu\text{m}$, $\Delta t = 1e-5$ s, and $\Delta T_{pc} = 0.4$ K or 0.2 K. Decreasing ΔT_{pc} from 0.4 K to 0.2 K increases the accuracy the temperature field on in the solid phase, but decreases the accuracy of the temperature field in the liquid phase.

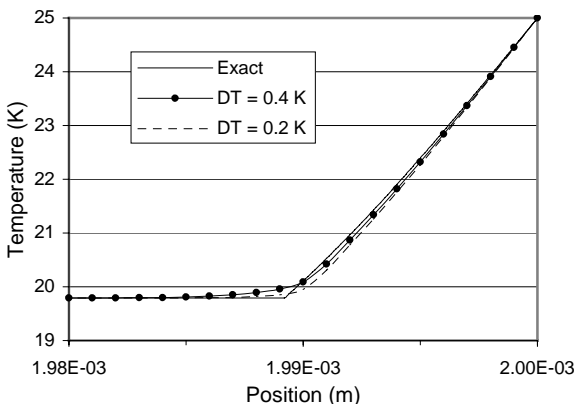


Figure 4. The effect of ΔT_{pc} on the accuracy of the temperature field.

To obtain accurate results using the apparent c_p method it is imperative that the time step is small enough that any node temperature does not skip the phase change interval, ΔT_{pc} , in one time step; otherwise, phase change will be neglected. In general, as the node spacing (Δr) and ΔT_{pc} are decreased the time step must also be decreased.

Target analysis

The integrated thermomechanical model described above was employed to evaluate the potential of several direct drive target designs. Of particular interest in this study is the evaluation of the potential of allowing phase change. The performances of other design options are briefly summarized to provide a basis for evaluating the potential of allowing phase change. For consistency each case is evaluated for a time of flight of 16.3 ms. This time of flight corresponds to target traveling through a reaction chamber of radius 6.5 m, at a velocity of 400 m/s.

Decreasing the initial target temperature

Perhaps the simplest method of increasing the robustness of a direct drive target is to decrease the initial temperature of the basic target (see fig. 1). Unfortunately, as the temperature of the DT solid is decreased thermal contraction and DT surface roughness could become problematic [18].

To study the influence of the initial target temperature on a basic target, it is assumed that the maximum DT temperature must remain below $T_{DT,TP}$.

Taking the required survival time to be 16.3 ms, the model predicts that decreasing the target temperature from 18 K to 16 K increases the maximum acceptable heat flux from ~ 0.6 W/cm² to ~ 1.5 W/cm². The increase in acceptable heat flux is less pronounced when transitioning from 16 K to 14 K, where the acceptable heat flux is only increased to ~ 1.9 W/cm².

Insulating the target

An intuitive method for protecting the target is to insulate it with porous foam cover. The thickness and porosity of the insulator could be limited by economic, implosion physics, or structural robustness considerations.

For insulated targets, $T_{TP,DT}$ is assumed to be the maximum allowable DT temperature to ensure survival. The initial target temperature is taken to be 16 K in the cases considered in this paper. The effects of the foam insulator porosity and thickness, on the time to reach $T_{TP,DT}$, are shown in fig. 5.

Increasing the insulator thickness, and decreasing the insulator density (increasing in foam porosity), increases the maximum allowable heat flux for any given time to triple point (survival time). The results for a typical target without insulation, with an initial

temperature of 16 K, are plotted in fig. 5 for reference.

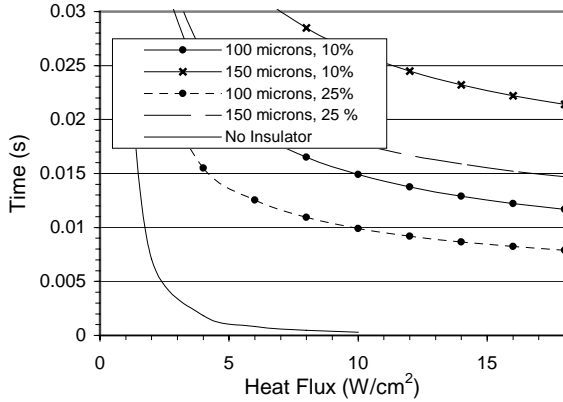


Figure 5. The time to reach the triple point for various insulated target configurations (16 K).

Melting only

Specific criteria for determining the viability of a target that has undergone melting are not known. Several possible limitations are:

1. Homogeneous nucleation.
2. The ultimate strength of the polymer or DT.
3. The melt layer thickness.

0.8T_c will be taken as the maximum allowable DT temperature before homogeneous nucleation. While the polymer shell will remain intact up to its ultimate strength, the DT solid could buckle before the ultimate strength is reached. The thickness of the acceptable melt is completely unknown.

Fig. 6 shows the time to reach several possible limiting factors for a target with an initial temperature of 16 K. In this case the maximum heat flux for a survival time of 16.3 ms, based on 0.8T_c, is 5.5 W/cm². The allowable heat fluxes for targets with initial temperatures of 14 K and 18 K are 5.7 W/cm² and 5.0 W/cm² respectively. For each initial temperature, homogeneous nucleation is the first limit to be exceeded. Allowing phase change has the maximum potential of more than tripling the allowable heat flux obtained using $T_{TP,DT}$ as the limit. The maximum allowable heat flux for a target undergoing phase change is two to three times less than the allowable heat flux for an insulated target.

The melting only scenario is certainly the best phase change scenario. However, due to the presence of a dissolved gas, and the possibility that preexisting nucleation sites, melting only is unlikely to occur.

By assuming that only melting occurs, much can be learned about the fertility of the liquid environment for nucleating and growing vapor bubbles. This can be evaluated by calculating the maximum superheat in the DT liquid. The superheat of a liquid is defined as:

$$\phi = T_{liq} - T_{sat} \quad (10)$$

where T_{liq} (K) is the maximum temperature in the liquid DT, and T_{sat} (K) is the saturation temperature of the

liquid at the liquid pressure. Most liquids require a minimum superheat of 2-3 K [20] for nucleation to occur. If the superheat is negative, then bubble nucleation and growth will not occur in a pure liquid.

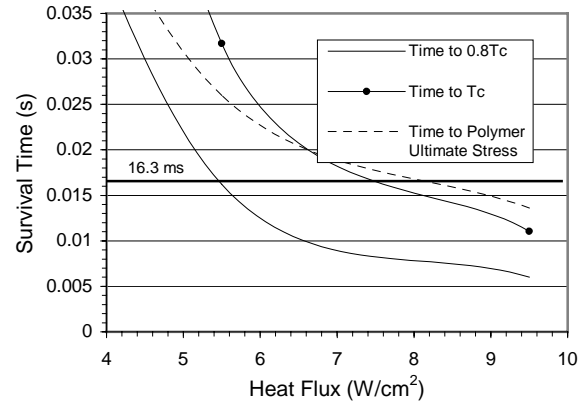


Figure 6. The survival of a 16 K basic target undergoing phase change.

For a basic target with an initial temperature of 16 K the superheat was found, using the integrated thermomechanical model, to be > 2-3 K for input heat fluxes higher than 2.5 W/cm². This suggests that homogeneous nucleation will likely occur for targets with initial temperatures of 16 K or higher.

Fig. 7 shows the superheat as a function of time for a basic target with an initial temperature of 14 K. When the incident heat flux is 2.5 W/cm² the superheat increases initially, then decreases to near zero for a short time, and then increases slowly. When the incident heat flux is decreased to 1 W/cm², the superheat increases for a very short time and then decreases to a negative value. These results suggest that the nucleation and growth of vapor bubbles will be less likely, or at a lower rate, for low incident heat fluxes.

Other cases were executed where the polymer shell thickness was increased. The increase in shell thickness decreased the superheat for each case. If a dissolved gas is present (i.e. helium-3), then the nucleation and growth of bubbles could still occur when the superheat is low or negative.

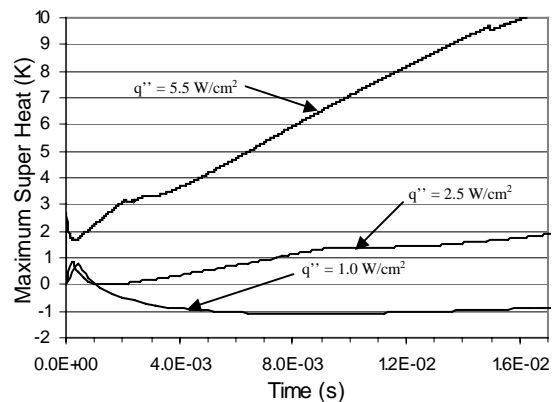


Figure 7. The superheat in a 14 K basic target experiencing melting.

Melting and Vaporization

To study the influence and behavior of DT vapor, it is assumed that a vapor layer initially exists between the DT solid and the polymer shell (fig. 2). The limiting criteria for this scenario could include:

1. The ultimate strength of the polymer or DT.
2. The vapor layer thickness.

Fig. 8 shows the time to reach the ultimate strength of the polymer as a function of heat flux, for a target with a 2- μm polymer shell. For a 2- μm shell the ultimate stress of the polymer is exceeded before the ultimate stress of the DT in every case. Based on the polymer ultimate strength, the maximum allowable heat fluxes at 16.3 ms are 2.1, 2.5, and 3.0 W/cm^2 for initial temperatures of 18, 16, and 14 K respectively. Note that the presence of vapor significantly decreased the allowable heat flux compared to the cases where only melting occurs. If a *vapor layer* is present, then allowing phase change only increases the acceptable heat flux 1.5 to 3 times the amount obtained by using $T_{TP,DT}$ as the limit.

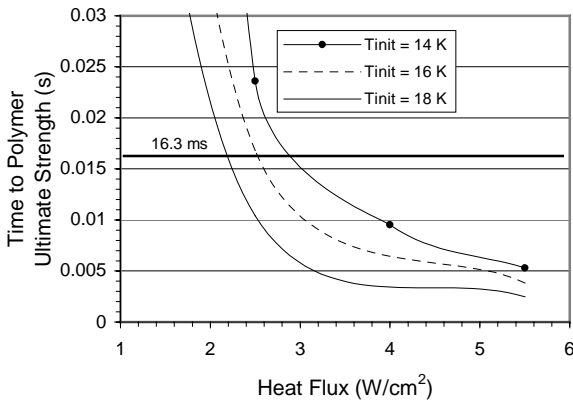


Figure 8. The time to reach the polymer ultimate strength when a vapor layer is present.

Basing target failure on the ultimate strength of the DT or polymer may be too hopeful. One must also consider the amount of vapor that is present. Fig. 9 shows the vapor layer thickness as a function of time for a target with an initial temperature of 18 K. The first thing to notice is that the vapor layer is initially 2- μm thick due to the saturation pressure of DT at 18 K. For the high heat flux cases the vapor layer grows rapidly and the ultimate strength of the polymer is exceeded before the nominal time of 16.3 ms is achieved.

Fig. 10 shows the vapor layer thickness for a target with a 2- μm shell thickness and an initial temperature of 14 K. A very interesting result occurs for this case when the input heat flux is 1 W/cm^2 ; the vapor layer thickness goes to zero. This result is very exciting since it suggests that vapor layers/bubbles could be eliminated or minimized under certain conditions.

Apparently this case exhibits vapor gap closure due to the low initial DT vapor pressure, and the low heat flux. For a target with an initial temperature of 16 K,

the model predicts that vapor closure can occur if the polystyrene shell thickness is increased to 10 μm .

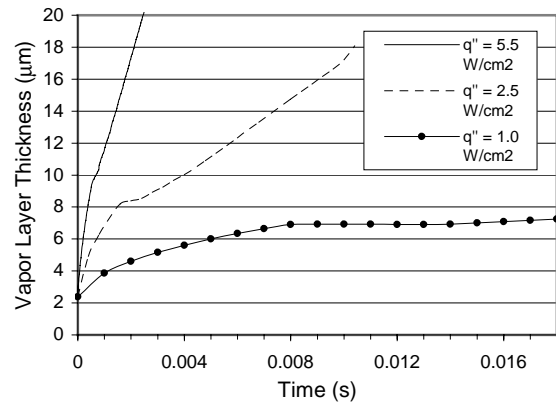


Figure 9. The vapor layer thickness as a function of time for a basic target, with an initial temperature of 18 K, experiencing vaporization.

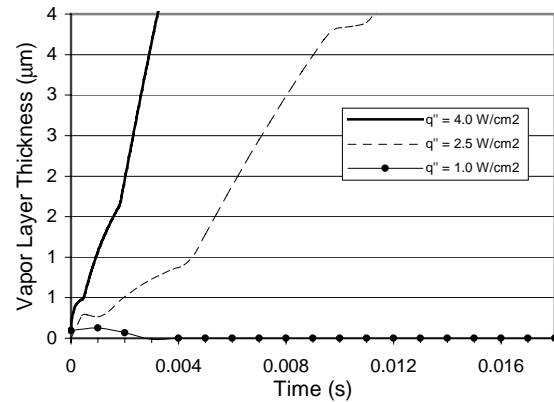


Figure 10. The vapor layer thickness as a function of time for a basic target, with an initial temperature of 14 K, experiencing vaporization.

Conclusions

The integrated thermomechanical model has been shown to be a valuable tool in predicting the response of an IFE direct drive target to an imposed heat flux. The model has been particularly useful for defining the maximum potential of basic and insulated targets, and targets that have undergone phase change.

This study has shown that a target that is allowed to experience phase change has the potential of increasing the allowable incident heat flux by 3+ times (for a target that experiences melting only) over the amount allowed by a basic target, but the allowable heat flux is only about one-half of the amount allowed by an insulated target. The simplicity of a phase change, compared to an insulated target, could still make it an attractive option. Using phase change and insulation would likely increase the allowable heat flux by an order of magnitude.

Major questions remain regarding the feasibility of allowing phase change. The main questions are related to the number and size of vapor bubbles, and their influence on the implosion efficiency. Future work will focus on numerically and experimentally determining the effects of phase change.

References

1. R. Cook, "Creating Microsphere Targets for Inertial Confinement Fusion Experiments," *Energy and Technology Review*, April 1995.
2. S. E. Bodner, D. G. Colombant, A. J. Schmitt, and M. Klapisch, "High-Gain Direct-Drive Target Design for Laser Fusion," *Physics of Plasmas*, 7(6), June 2000, pp. 2298-2301.
3. J. Grun, et al., "Rayleigh-Taylor Instability Growth Rates in Targets Accelerated with a Laser Beam Smoothed by Induced Spatial Incoherences," *Phys. Rev. Lett.* 58(25), June 1987, pp. 2672-2676.
4. C. J. Pawley, et al., "Observation of Rayleigh-Taylor growth to short wavelengths on NIKE," *Phys. Plasmas*, 6(2), February 1999, pp. 565-570.
5. J. P. Knauer, et al., "Single-mode, Rayleigh-Taylor growth-rate measurements on the OMEGA laser system," *Phys. Plasmas*, 7(1), January 2000.
6. R. W. Petzoldt, et al, "Direct drive target survival during injection in an inertial fusion energy power plant," *Nucl. Fusion*, Vol. 42, pp. 1351-1356, 2002.
7. N. P. Siegel, "Thermal Analysis of Inertial Fusion Energy Targets," Master of Science Thesis, San Diego State University, May 2000.
8. A. R. Raffray, J. Pulsifer, M. S. Tilack, "Target Thermal Response to Gas Interactions," UCSD Technical Report, UCSD-ENG-092, <http://aries.ucsd.edu/FERP/reports.shtml>.
9. P. C. Souers, *Hydrogen Properties for Fusion Energy*, University of California Press, Berkley, 1986.
10. K. Denpoh, "Modeling of Rarefied Gas Heat Conduction Between Wafer and Susceptor," *IEEE Transactions on Semiconductor Manufacturing*, 11(1), February 1998, pp. 25-29.
11. Y. A. Cengel and M. A. Boles, *Thermodynamics an Engineering Approach*, WCB/McGraw-Hill, Boston, 1998.
12. M. N. Özisik, *Finite Difference Methods in Heat Transfer*, CRC Press, Boca Raton, 1994.
13. J.G. Collier, *Convective Boiling and Condensation*, p. 317-322, McGraw-Hill International Book Co., New York; London, 1981.
14. A. C. Ugural, *Stresses in Plates and Shells*, WCB/McGraw Hill, Boston, 1999.
15. W. C. Young, *Roark's Formulas for Stress & Strain*, McGraw-Hill, New York, 1989, p. 640.
16. C. Bonacina, et. al., "Numerical Solution of Phase-Change Problems," *Int. J. Heat Mass Transfer*, Vol. 16, pp. 1825-1832, 1973.
17. M. N. Özisik, *Heat Conduction*, Wiley, New York, 1993.
18. J. Hoffer, "Update on Solid DT Studies," Presentation given at the April 2002 HAPL meeting, <http://aries.ucsd.edu/HAPL/MEETINGS/0304-HAPL/hoffer.ppt>.
19. S. G. Kandlikar, M. Shoji, V. K. Dhir, *Handbook of Phase Change*, Taylor & Francis, Philadelphia, PA, 1999.
20. S. Van Stralen, R. Cole, *Boiling Phenomena*, Hemisphere Publishing Corp., Washington, 1979.